National Semiconductor is now part of

Texas Instruments.

Search http://www.ti.com/ for the latest technical

information and details on our current products and services.

National Semiconductor

July 23, 2009

LMP2021/LMP2022

Zero Drift, Low Noise, EMI Hardened Amplifiers

General Description

The LMP2021/LMP2022 are single and dual precision operational amplifiers offering ultra low input offset voltage, near zero input offset voltage drift, very low input voltage noise and very high open loop gain. They are part of the LMP® precision family and are ideal for instrumentation and sensor interfaces.

The LMP2021/LMP2022 have only 0.004 µV/°C of input offset voltage drift, and 0.4 µV of input offset voltage. These attributes provide great precision in high accuracy applications.

The proprietary continuous correction circuitry guarantees impressive CMRR and PSRR, removes the 1/f noise component, and eliminates the need for calibration in many circuits.

With only 260 nV_{PP} (0.1 Hz to 10 Hz) of input voltage noise and no 1/f noise component, the LMP2021/LMP2022 are suitable for low frequency applications such as industrial precision weigh scales. The low input bias current of 23 pA makes these excellent choices for high source impedance circuits such as non-invasive medical instrumentation as well as test and measurement equipment. The extremely high open loop gain of 160 dB drastically reduces gain error in high gain applications. With ultra precision DC specifications and very low noise, the LMP2021/LMP2022 are ideal for position sensors, bridge sensors, pressure sensors, medical equipment and other high accuracy applications with very low error budgets.

The LMP2021 is offered in 5-Pin SOT-23 and 8-Pin SOIC packages. The LMP2022 is offered in 8-Pin MSOP and 8-Pin SOIC packages.

Features

(Typical Values, T_A = 25°C, V_S = 5V)

- Input offset voltage (typical) –0.4 µV
- Input offset voltage (max) ±5 µV
- Input offset voltage drift (typical) -0.004 µV/°C
- Input offset voltage drift (max) ±0.02 µV/°C
- Input voltage noise, A_V = 1000 11 nV/√Hz
- Open loop gain 160 dB
- CMRR 139 dB
- PSRR 130 dB
- Supply voltage range 2.2V to 5.5V
- Supply current (per amplifier) 1.1 mA
- Input bias current ±25 pA
- GBW 5 MHz
- Slew rate 2.6 V/µs
- Operating temperature range –40°C to 125°C
- 5-Pin SOT-23, 8-Pin MSOP and 8-Pin SOIC Packages

Applications

- Precision instrumentation amplifiers
- Battery powered instrumentation
- Thermocouple amplifiers
- Bridge amplifiers

Typical Application

Bridge Amplifier

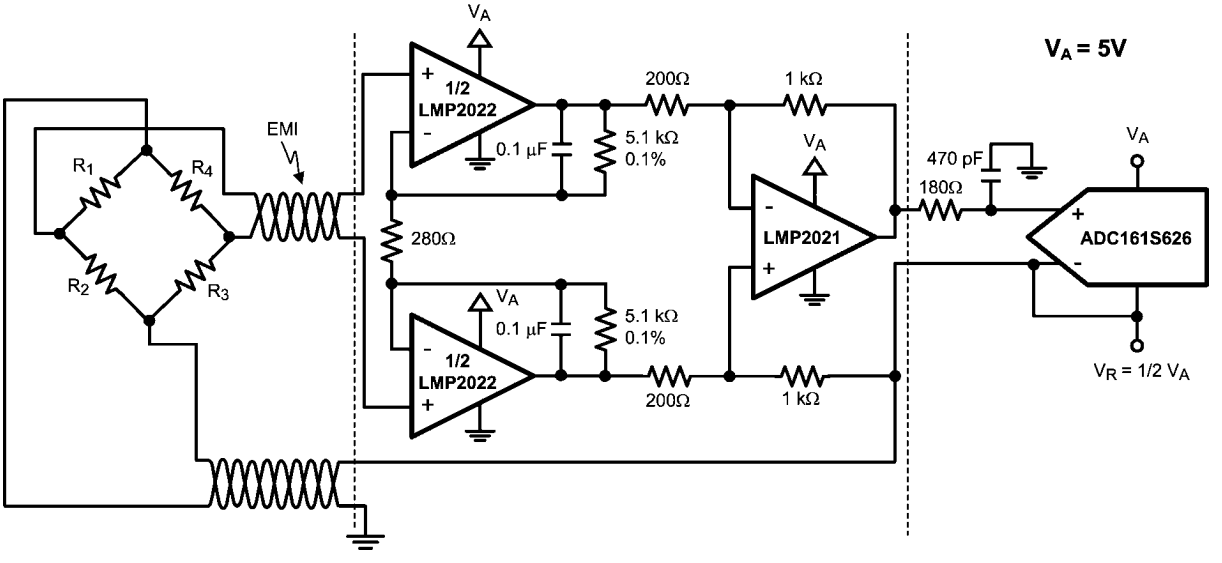

30014972

The LMP2021/LMP2022 support systems with up to 24 bits of accuracy.

LMP® is a registered trademark of National Semiconductor Corporation.

Absolute Maximum Ratings (Note 1)

If Military/Aerospace specified devices are required, please contact the National Semiconductor Sales Office/ Distributors for availability and specifications.

ESD Tolerance (Note 2)	
Human Body Model	2000V
Machine Model	200V
Charge Device Model	1000V
V_{IN} Differential	$\pm V_S$
Supply Voltage ($V_S = V^+ - V^-$)	6.0V
All Other Pins	$V^+ + 0.3V$, $V^- - 0.3V$
Output Short-Circuit Duration to V^+ or V^- (Note 3)	5s
Storage Temperature Range	−65°C to 150°C
Junction Temperature (Note 4)	150°C max
Soldering Information	
Infrared or Convection (20 sec)	235°C
Wave Soldering Lead Temperature (10 sec)	260°C

Operating Ratings (Note 1)

Temperature Range	−40°C to 125°C
Supply Voltage ($V_S = V^+ - V^-$)	2.2V to 5.5V
Package Thermal Resistance (θ_{JA})	
5-Pin SOT-23	164 °C/W
8-Pin SOIC (LMP2021)	106 °C/W
8-Pin SOIC (LMP2022)	106 °C/W
8-Pin MSOP	217 °C/W

2.5V Electrical Characteristics (Note 5)

Unless otherwise specified, all limits are guaranteed for T_A = 25°C, V^+ = 2.5V, V^- = 0V, $V_{CM} = V^+/2$, R_L >10 kΩ to $V^+/2$. **Boldface** limits apply at the temperature extremes.

Symbol	Parameter	Conditions	Min (Note 7)	Typ (Note 6)	Max (Note 7)	Units
V_{OS}	Input Offset Voltage			−0.9	±5 **±10**	µV
TCV_{OS}	Input Offset Voltage Drift (Note 8)			0.001	±0.02	µV/°C
I_B	Input Bias Current			±23	±100 **±300**	pA
I_{OS}	Input Offset Current			±57	±200 **±250**	pA
CMRR	Common Mode Rejection Ratio	−0.2V ≤ V_{CM} ≤ 1.7V 0V ≤ V_{CM} ≤ 1.5V	105 **102**	141		dB
CMVR	Input Common-Mode Voltage Range	Large Signal CMRR ≥ 105 dB Large Signal CMRR ≥ 102 dB	−0.2 **0**		1.7 **1.5**	V
EMIRR	Electro-Magnetic Interference Rejection Ratio (Note 9)	IN+ and IN−: $V_{RF\text{-}PEAK}$ = 100 mV_P (−20 dBV_P), f = 400 MHz		40		dB
		IN+ and IN−: $V_{RF\text{-}PEAK}$ = 100 mV_P (−20 dBV_P), f = 900 MHz		48		
		IN+ and IN−: $V_{RF\text{-}PEAK}$ = 100 mV_P (−20 dBV_P), f = 1800 MHz		67		
		IN+ and IN−: $V_{RF\text{-}PEAK}$ = 100 mV_P (−20 dBV_P), f = 2400 MHz		79		
PSRR	Power Supply Rejection Ratio	2.5V ≤ V^+ ≤ 5.5V, V_{CM} = 0	115 **112**	130		dB
		2.2V ≤ V^+ ≤ 5.5V, V_{CM} = 0	110	130		
A_{VOL}	Large Signal Voltage Gain	R_L = 10 kΩ to $V^+/2$ V_{OUT} = 0.5V to 2V	124 **119**	150		dB
		R_L = 2 kΩ to $V^+/2$ V_{OUT} = 0.5V to 2V	120 **115**	150		

Symbol	Parameter	Conditions	Min (Note 7)	Typ (Note 6)	Max (Note 7)	Units
V_{OUT}	Output Swing High	R_L = 10 kΩ to V+/2		38	50 **70**	mV from either rail
		R_L = 2 kΩ to V+/2		62	85 **115**	
	Output Swing Low	R_L = 10 kΩ to V+/2		30	45 **55**	
		R_L = 2 kΩ to V+/2		58	75 **95**	
I_{OUT}	Linear Output Current	Sourcing, V_{OUT} = 2V	30	50		mA
		Sinking, V_{OUT} = 0.5V	30	50		
I_S	Supply Current	Per Amplifier		0.95	1.10 **1.37**	mA
SR	Slew Rate (Note 10)	A_V = +1, C_L = 20 pF, R_L = 10 kΩ V_O = 2 V_{PP}		2.5		V/µs
GBW	Gain Bandwidth Product	C_L = 20 pF, R_L = 10 kΩ		5		MHz
G_M	Gain Margin	C_L = 20 pF, R_L = 10 kΩ		10		dB
Φ_M	Phase Margin	C_L = 20 pF, R_L = 10 kΩ		60		deg
C_{IN}	Input Capacitance	Common Mode		12		pF
		Differential Mode		12		
e_n	Input-Referred Voltage Noise Density	f = 0.1 kHz or 10 kHz, A_V = 1000		11		$nV/\sqrt{Hz}$
		f = 0.1 kHz or 10 kHz, A_V = 100		15		
	Input-Referred Voltage Noise	0.1 Hz to 10 Hz		260		nV_{PP}
		0.01 Hz to 10 Hz		330		
i_n	Input-Referred Current Noise	f = 1 kHz		350		$fA/\sqrt{Hz}$
t_r	Recovery time	to 0.1%, R_L = 10 kΩ, A_V = −50, V_{OUT} = 1.25 V_{PP} Step, Duration = 50 µs		50		µs
CT	Cross Talk	LMP2022, f = 1 kHz		150		dB

5V Electrical Characteristics (Note 5)

Unless otherwise specified, all limits are guaranteed for T_A = 25°C, V+ = 5V, V− = 0V, V_{CM} = V+/2, R_L > 10 kΩ to V+/2. **Boldface** limits apply at the temperature extremes.

Symbol	Parameter	Conditions	Min (Note 7)	Typ (Note 6)	Max (Note 7)	Units
V_{OS}	Input Offset Voltage			−0.4	±5 **±10**	µV
TCV_{OS}	Input Offset Voltage Drift (Note 8)			−0.004	±0.02	µV/°C
I_B	Input Bias Current			±25	±100 **±300**	pA
I_{OS}	Input Offset Current			±48	±200 **±250**	pA
CMRR	Common Mode Rejection Ratio	−0.2V ≤ V_{CM} ≤ 4.2V 0V ≤ V_{CM} ≤ 4.0V	120 **115**	139		dB
CMVR	Input Common-Mode Voltage Range	Large Signal CMRR ≥ 120 dB Large Signal CMRR ≥ 115 dB	−0.2 **0**		4.2 **4.0**	V

Symbol	Parameter	Conditions		Min (Note 7)	Typ (Note 6)	Max (Note 7)	Units
EMIRR	Electro-Magnetic Interference Rejection Ratio (Note 9)	IN+ and IN–	$V_{RF-PEAK}$ = 100 mV_P (–20 dBV_P) f = 400 MHz		58		dB
			$V_{RF-PEAK}$ = 100 mV_P (–20 dBV_P) f = 900 MHz		64		
			$V_{RF-PEAK}$ = 100 mV_P (–20 dBV_P) f = 1800 MHz		72		
			$V_{RF-PEAK}$ = 100 mV_P (–20 dBV_P) f = 2400 MHz		82		
PSRR	Power Supply Rejection Ratio	2.5V ≤ V^+ ≤ 5.5V, V_{CM} = 0		115 **112**	130		dB
		2.2V ≤ V^+ ≤ 5.5V, V_{CM} = 0		110	130		
A_{VOL}	Large Signal Voltage Gain	R_L = 10 kΩ to V^+/2 V_{OUT} = 0.5V to 4.5V		125 **120**	160		dB
		R_L = 2 kΩ to V^+/2 V_{OUT} = 0.5V to 4.5V		123 **118**	160		
V_{OUT}	Output Swing High	R_L = 10 kΩ to V^+/2			83	135 **170**	mV from either rail
		R_L = 2 kΩ to V^+/2			120	160 **204**	
	Output Swing Low	R_L = 10 kΩ to V^+/2			65	80 **105**	
		R_L = 2 kΩ to V^+/2			103	125 **158**	
I_{OUT}	Linear Output Current	Sourcing, V_{OUT} = 4.5V		30	50		mA
		Sinking, V_{OUT} = 0.5V		30	50		
I_S	Supply Current	Per Amplifier			1.1	1.25 **1.57**	mA
SR	Slew Rate (Note 10)	A_V = +1, C_L = 20 pF, R_L = 10 kΩ V_O = 2 V_{PP}			2.6		V/µs
GBW	Gain Bandwidth Product	C_L = 20 pF, R_L = 10 kΩ			5		MHz
G_M	Gain Margin	C_L = 20 pF, R_L = 10 kΩ			10		dB
Φ_M	Phase Margin	C_L = 20 pF, R_L = 10 kΩ			60		deg
C_{IN}	Input Capacitance	Common Mode			12		pF
		Differential Mode			12		
e_n	Input-Referred Voltage Noise Density	f = 0.1 kHz or 10 kHz, A_V= 1000			11		$nV/\sqrt{Hz}$
		f = 0.1 kHz or 10 kHz, A_V= 100			15		
	Input-Referred Voltage Noise	0.1 Hz to 10 Hz Noise			260		nV_{PP}
		0.01 Hz to 10 Hz Noise			330		
i_n	Input-Referred Current Noise	f = 1 kHz			350		$fA/\sqrt{Hz}$
t_r	Input Overload Recovery time	to 0.1%, R_L = 10 kΩ, A_V = –50, V_{OUT} = 2.5 V_{PP} Step, Duration = 50 µs			50		µs
CT	Cross Talk	LMP2022, f = 1 kHz			150		dB

Note 1: Absolute Maximum Ratings indicate limits beyond which damage to the device may occur. Operating Ratings indicate conditions for which the device is intended to be functional, but specific performance is not guaranteed. For guaranteed specifications and the test conditions, see the Electrical Characteristics Tables.

Note 2: Human Body Model per MIL-STD-883, Method 3015.7. Machine Model, per JESD22-A115-A. Field-Induced Charge-Device Model, per JESD22-C101-C.

Note 3: Package power dissipation should be observed.

Note 4: The maximum power dissipation is a function of $T_{J(MAX)}$, θ_{JA}, and T_A. The maximum allowable power dissipation at any ambient temperature is $P_D = (T_{J(MAX)} - T_A)/ \theta J_A$. All numbers apply for packages soldered directly onto a PC board.

Note 5: Electrical Table values apply only for factory testing conditions at the temperature indicated. Factory testing conditions result in very limited self-heating of the device such that $T_J = T_A$. No guarantee of parametric performance is indicated in the electrical tables under conditions of internal self-heating where $T_J > T_A$.

Note 6: Typical values represent the most likely parametric norm at the time of characterization. Actual typical values may vary over time and will also depend on the application and configuration. The typical values are not tested and are not guaranteed on shipped production material.

Note 7: All limits are guaranteed by testing, statistical analysis or design.

Note 8: Offset voltage temperature drift is determined by dividing the change in V_{OS} at the temperature extremes by the total temperature change.

Note 9: The EMI Rejection Ratio is defined as EMIRR = 20Log ($V_{R_{F-PEAK}}/\Delta V_{OS}$).

Note 10: The number specified is the average of rising and falling slew rates and is measured at 90% to 10%.

Connection Diagrams

5-Pin SOT-23

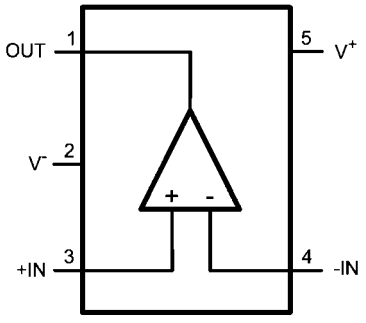

30014902

Top View

8-Pin SOIC (LMP2021)

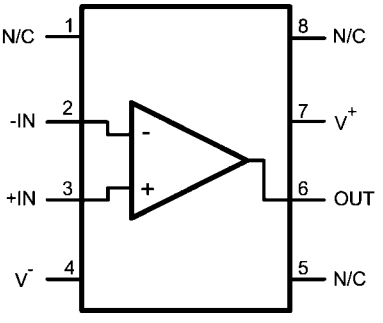

30014953

Top View

8-Pin SOIC/MSOP (LMP2022)

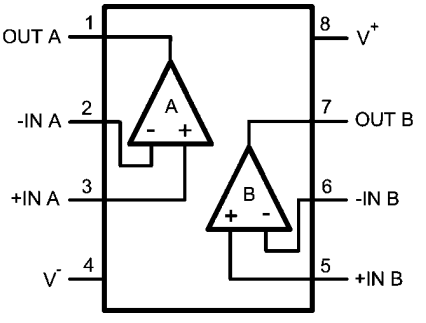

30014903

Ordering Information

Package	Part Number	Package Marking	Transport Media	NSC Drawing
5-Pin SOT-23	LMP2021MF	AF5A	1k Units Tape and Reel	MF05A
	LMP2021MFE		250 Units Tape and Reel	
	LMP2021MFX		3k Units Tape and Reel	
8-Pin SOIC	LMP2021MA	LMP2021MA	95 Units/Rail	M08A
	LMP2021MAX		2.5k Units Tape and Reel	
	LMP2022MA	LMP2022MA	95 Units/Rail	
	LMP2022MAX		2.5k Units Tape and Reel	
8-Pin MSOP	LMP2022MM	AV5A	1k Units Tape and Reel	MUA08A
	LMP2022MME		250 Units Tape and Reel	
	LMP2022MMX		3.5k Units Tape and Reel	

Typical Performance Characteristics

Unless otherwise noted: T_A = 25°C, R_L > 10 kΩ, V_S= V^+ – V^-, V_S= 5V, V_{CM} = V_S/2.

Offset Voltage Distribution

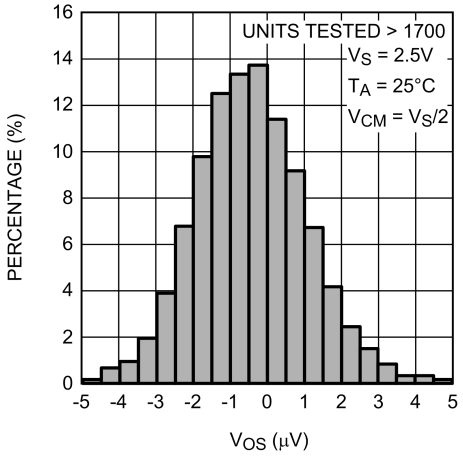

30014912

TCV_{OS} Distribution

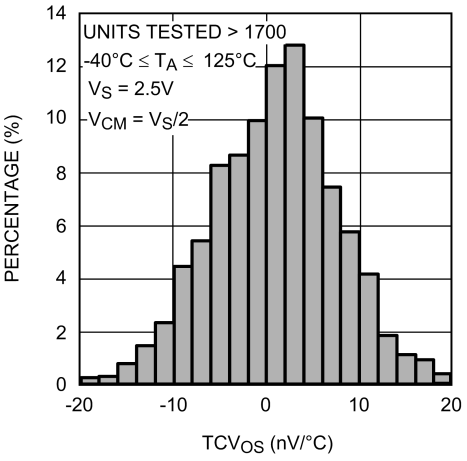

30014914

Offset Voltage Distribution

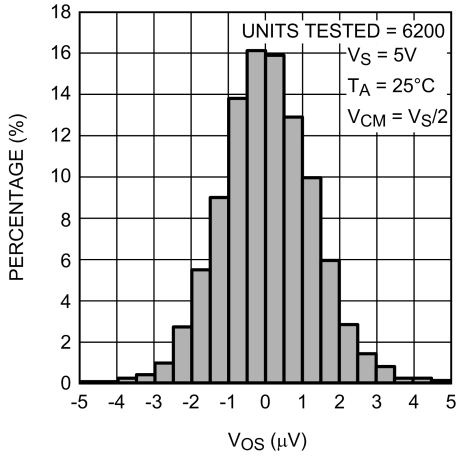

30014913

TCV_{OS} Distribution

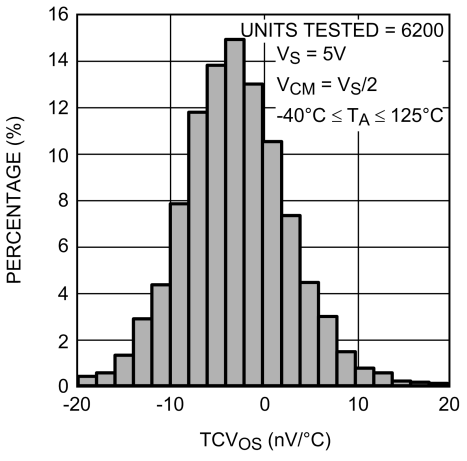

30014915

Offset Voltage vs. Supply Voltage

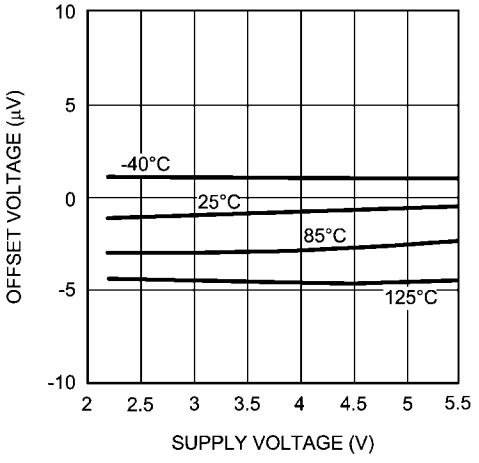

30014905

PSRR vs. Frequency

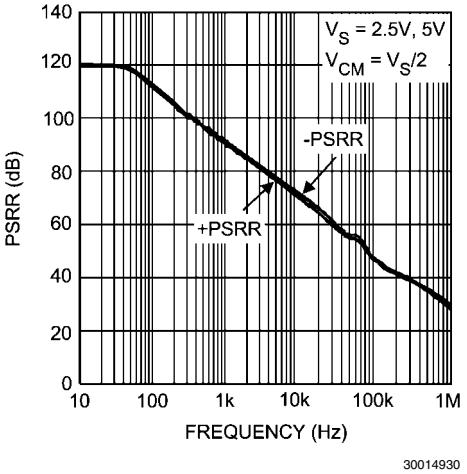

30014930

Input Bias Current vs. V_{CM}

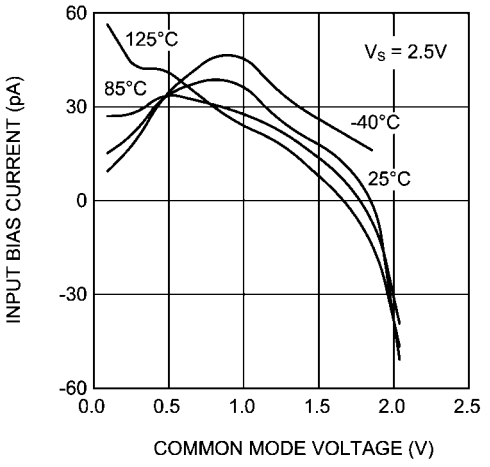

30014962

Input Bias Current vs. V_{CM}

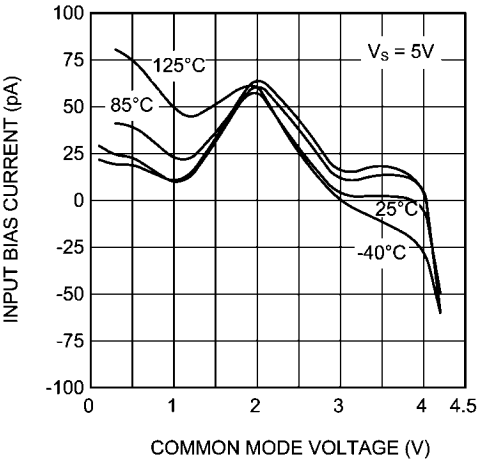

30014961

Offset Voltage vs. V_{CM}

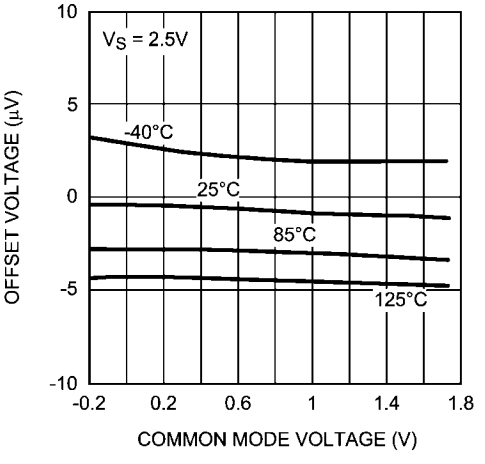

30014906

Offset Voltage vs. V_{CM}

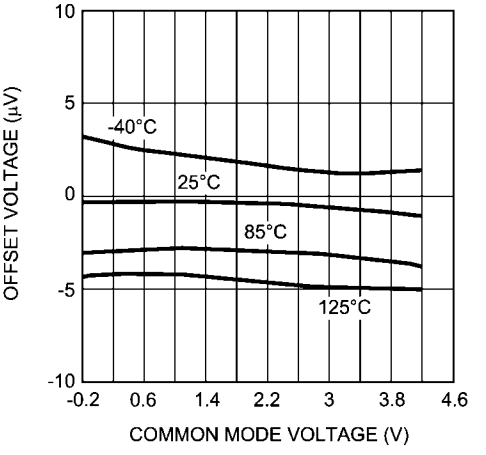

30014907

Supply Current vs. Supply Voltage (Per Amplifier)

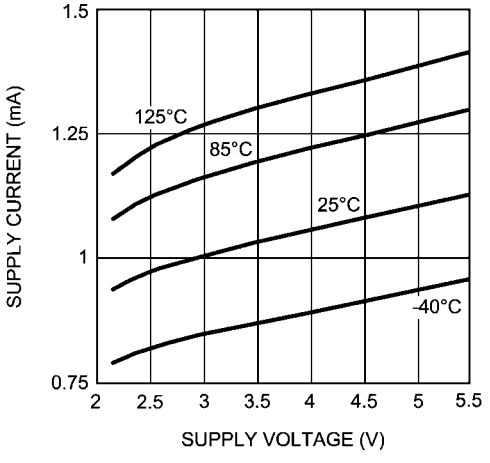

30014904

Input Voltage Noise vs. Frequency

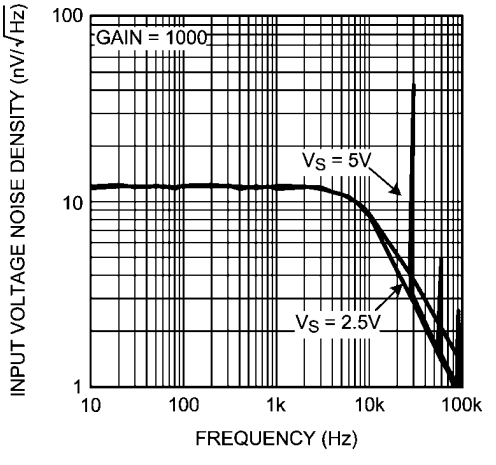

30014926

Open Loop Frequency Response

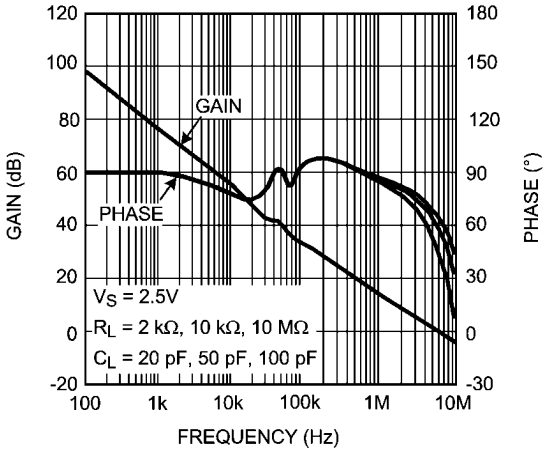

30014922

Open Loop Frequency Response

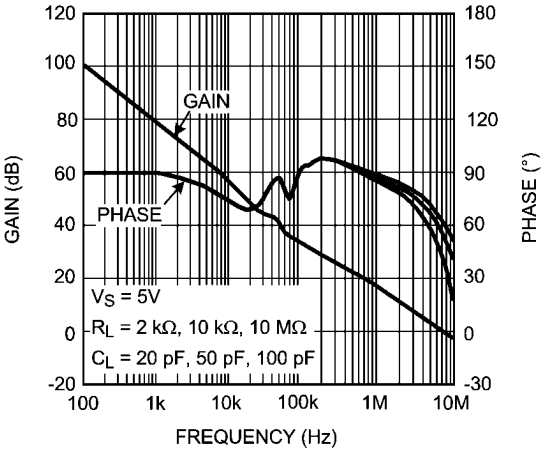

30014921

Open Loop Frequency Response Over Temperature

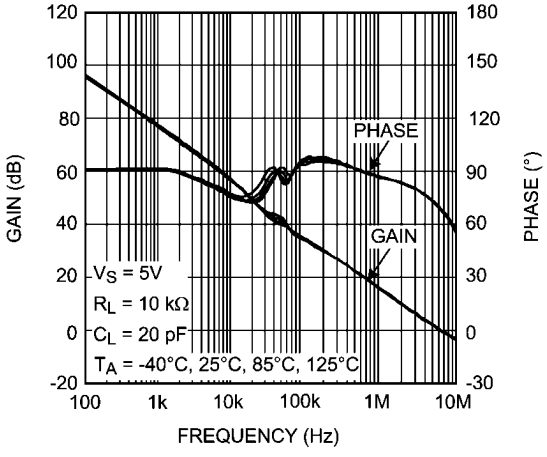

30014923

EMIRR vs. Frequency

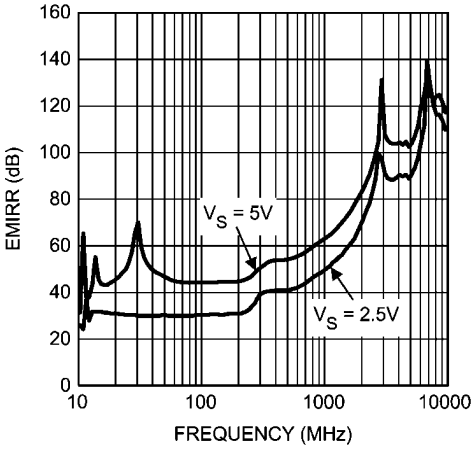

30014934

EMIRR vs. Input Power

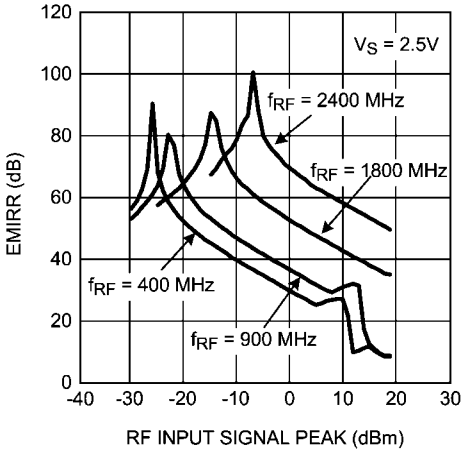

30014932

EMIRR vs. Input Power

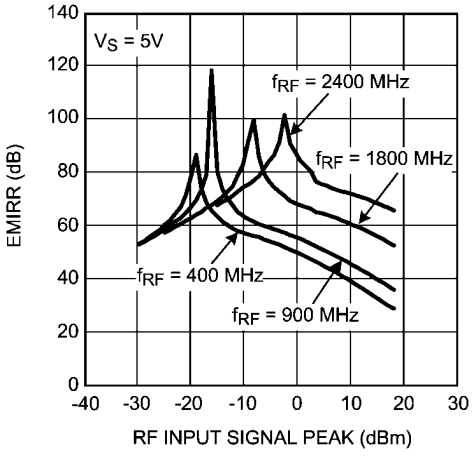

30014933

Time Domain Input Voltage Noise

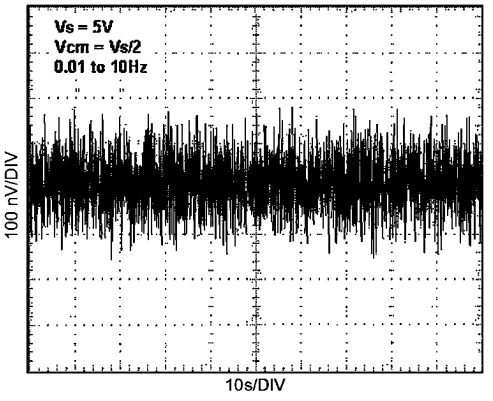

30014928

Time Domain Input Voltage Noise

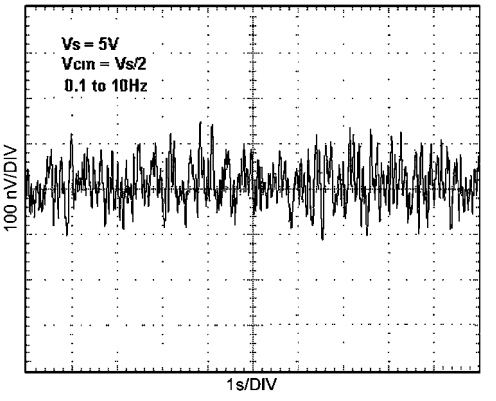

30014929

CMRR vs. Frequency

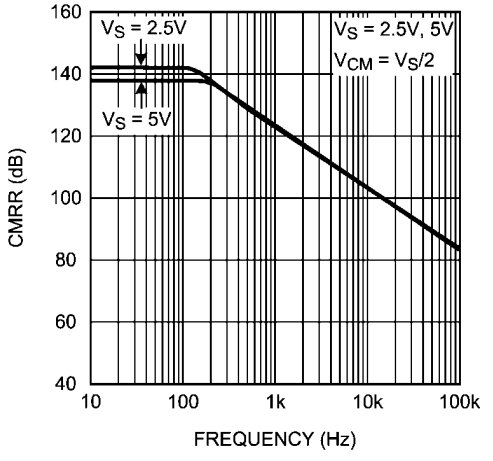

30014931

Slew Rate vs. Supply Voltage

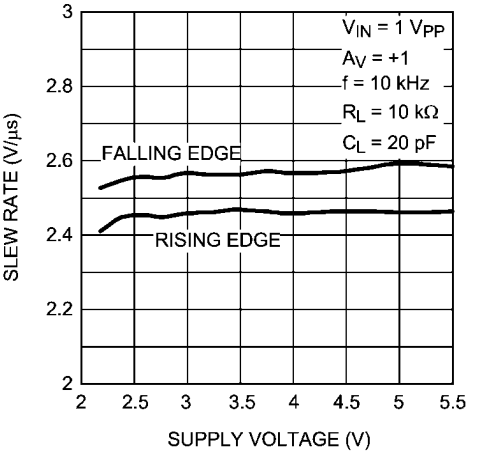

30014916

Output Swing High vs. Supply Voltage

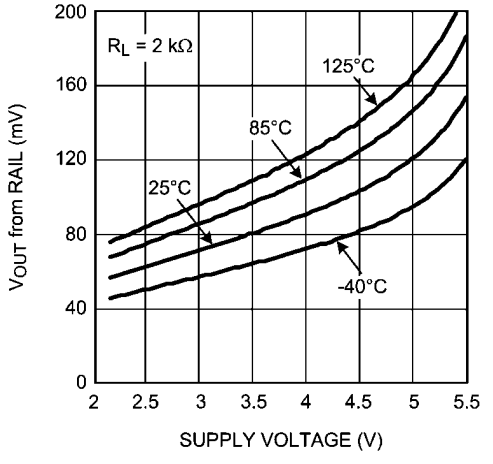

30014909

Output Swing Low vs. Supply Voltage

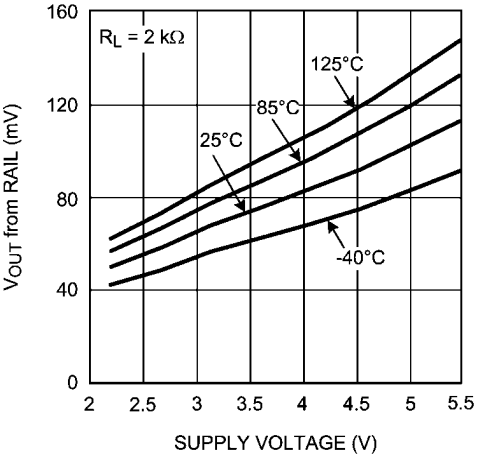

30014911

Output Swing High vs. Supply Voltage

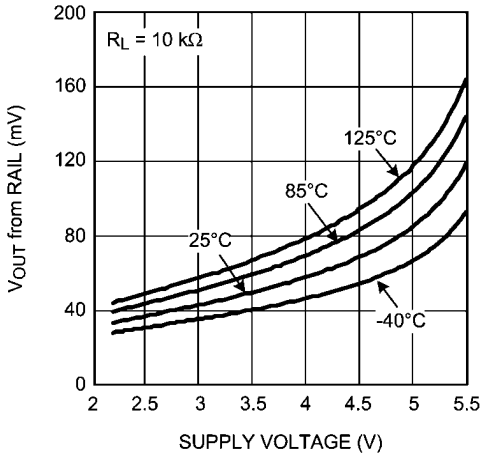

30014908

Output Swing Low vs. Supply Voltage

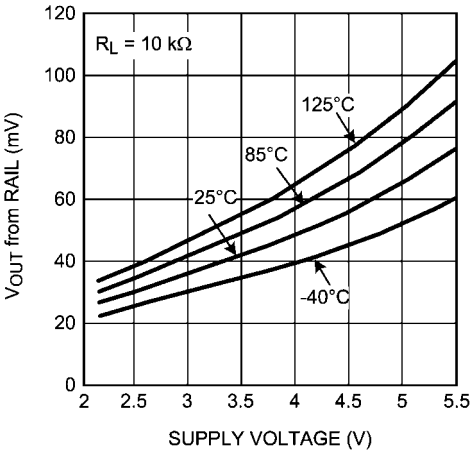

30014910

Overload Recovery Time

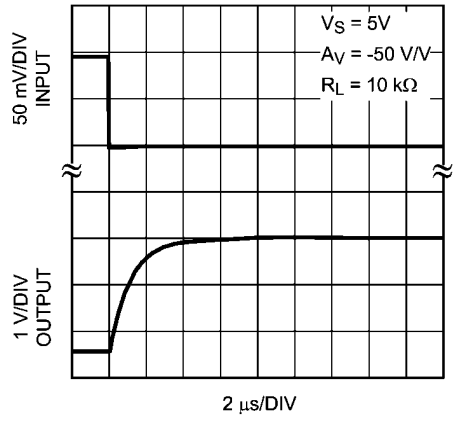

30014942

Overload Recovery Time

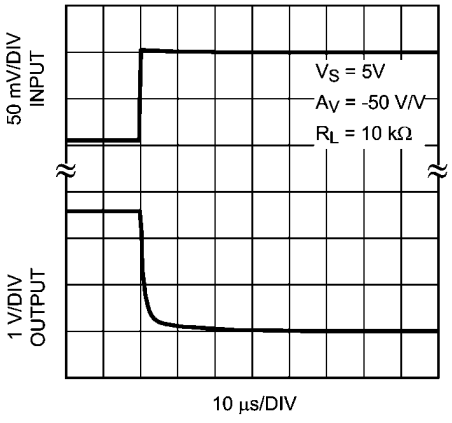

30014943

Large Signal Step Response

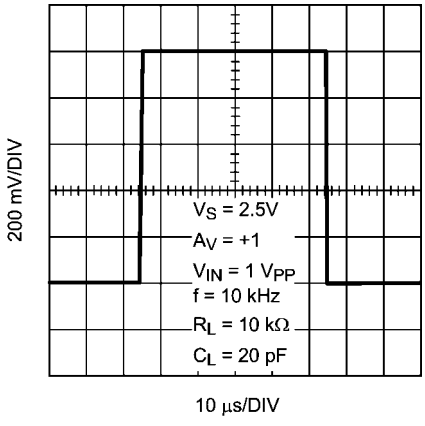

30014920

Small Signal Step Response

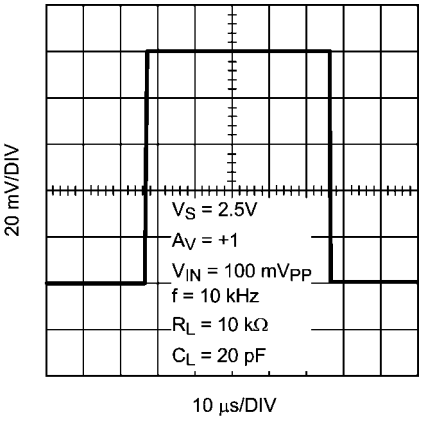

30014918

Large Signal Step Response

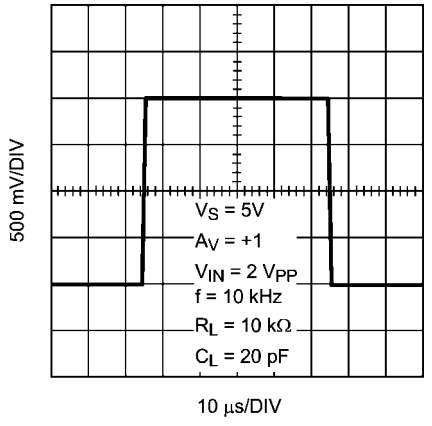

30014919

Small Signal Step Response

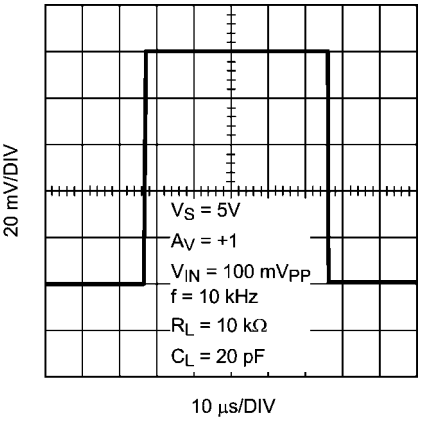

30014917

Output Voltage vs. Output Current

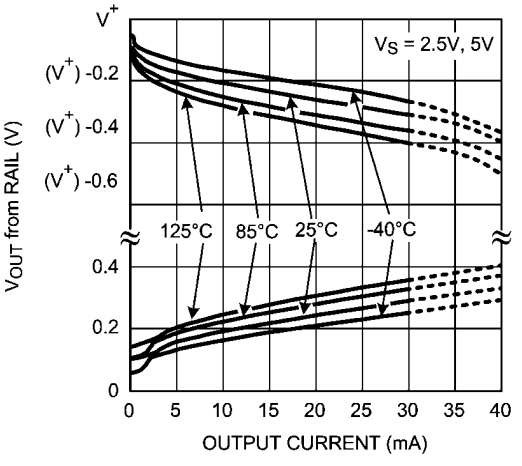

30014924

Cross Talk Rejection Ratio vs. Frequency (LMP2022)

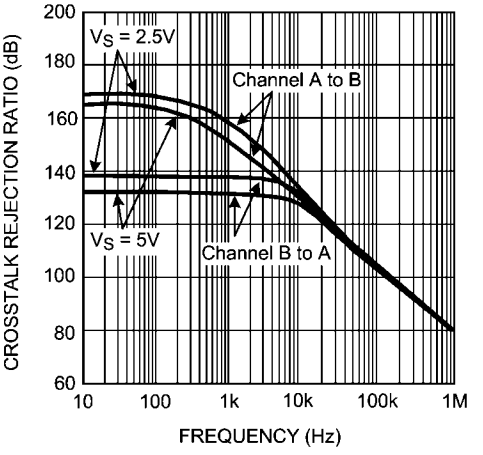

30014973

Application Information

LMP2021/LMP2022

The LMP2021/LMP2022 are single and dual precision operational amplifiers with ultra low offset voltage, ultra low offset voltage drift, and very low input voltage noise with no 1/f and extended supply voltage range. The LMP2021/LMP2022 offer on chip EMI suppression circuitry which greatly enhances the performance of these precision amplifiers in the presence of radio frequency signals and other disturbances.

The LMP2021/LMP2022 utilize proprietary techniques to measure and continuously correct the input offset error voltage. The LMP2021/LMP2022 have a DC input offset voltage with a maximum value of ±5 µV and an input offset voltage drift maximum value of 0.02 µV/°C. The input voltage noise of the LMP2021/LMP2022 is less than 11 nV/$\sqrt{\text{Hz}}$ at a voltage gain of 1000 V/V and has no flicker noise component. This makes the LMP2021/LMP2022 ideal for high accuracy, low frequency applications where lots of amplification is needed and the input signal has a very small amplitude.

The proprietary input offset correction circuitry enables the LMP2021/LMP2022 to have superior CMRR and PSRR performances. The combination of an open loop voltage gain of 160 dB, CMRR of 142 dB, PSRR of 130 dB, along with the ultra low input offset voltage of only –0.4 µV, input offset voltage drift of only –0.004 µV/°C, and input voltage noise of only 260 nV_{PP} at 0.1 Hz to 10 Hz make the LMP2021/LMP2022 great choices for high gain transducer amplifiers, ADC buffer amplifiers, DAC I-V conversion, and other applications requiring precision and long-term stability. Other features are rail-to-rail output, low supply current of 1.1 mA per amplifier, and a gain-bandwidth product of 5 MHz.

The LMP2021/LMP2022 have an extended supply voltage range of 2.2V to 5.5V, making them ideal for battery operated portable applications. The LMP2021 is offered in 5-pin SOT-23 and 8-pin SOIC packages. The LMP2022 is offered in 8-pin MSOP and 8-Pin SOIC packages.

EMI SUPPRESSION

The near-ubiquity of cellular, bluetooth, and Wi-Fi signals and the rapid rise of sensing systems incorporating wireless radios make electromagnetic interference (EMI) an evermore important design consideration for precision signal paths. Though RF signals lie outside the op amp band, RF carrier switching can modulate the DC offset of the op amp. Also some common RF modulation schemes can induce down-converted components. The added DC offset and the induced signals are amplified with the signal of interest and thus corrupt the measurement. The LMP2021/LMP2022 use on chip filters to reject these unwanted RF signals at the inputs and power supply pins; thereby preserving the integrity of the precision signal path.

Twisted pair cabling and the active front-end's common-mode rejection provide immunity against low frequency noise (i.e. 60 Hz or 50 Hz mains) but are ineffective against RF interference. *Figure 12* displays this. Even a few centimeters of PCB trace and wiring for sensors located close to the amplifier can pick up significant 1 GHz RF. The integrated EMI filters of LMP2021/LMP2022 reduce or eliminate external shielding and filtering requirements, thereby increasing system robustness. A larger EMIRR means more rejection of the RF interference. For more information on EMIRR, please refer to AN-1698.

INPUT VOLTAGE NOISE

The input voltage noise density of the LMP2021/LMP2022 has no 1/f corner, and its value depends on the feedback network used. This feature of the LMP2021/LMP2022 differentiates this family from other products currently available from other vendors. In particular, the input voltage noise density decreases as the closed loop voltage gain of the LMP2021/LMP2022 increases. The input voltage noise of the LMP2021/LMP2022 is less than 11 nV/$\sqrt{\text{Hz}}$ when the closed loop voltage gain of the op amp is 1000. Higher voltage gains are required for smaller input signals. When the input signal is smaller, a lower input voltage noise is quite advantageous and increases the signal to noise ratio.

Figure 1 shows the input voltage noise of the LMP2021/LMP2022 as the closed loop gain increases.

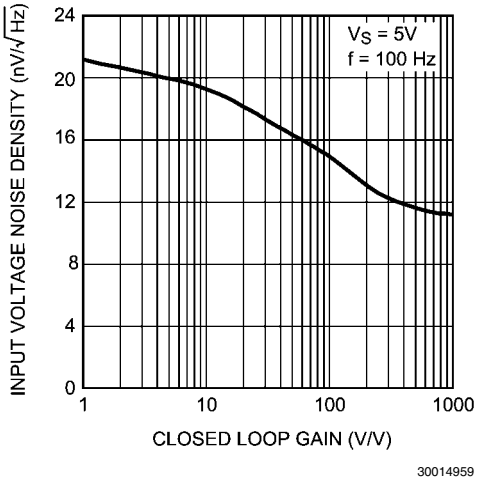

FIGURE 1. Input Voltage Noise Density decreases with Gain

Figure 2 shows the input voltage noise density does not have the 1/f component.

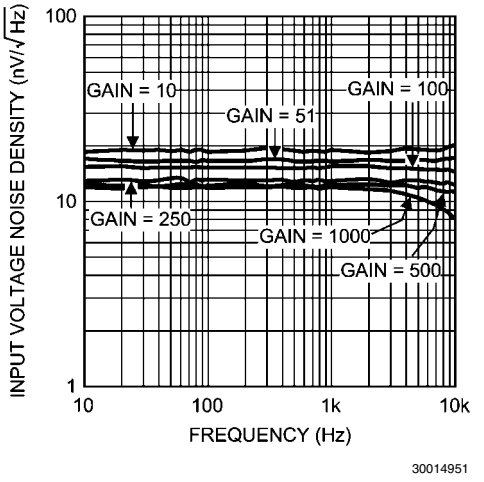

FIGURE 2. Input Voltage Noise Density with no 1/f

With smaller and smaller input signals and high precision applications with lower error budget, the reduced input voltage noise and no 1/f noise allow more flexibility in circuit design.

ACHIEVING LOWER NOISE WITH FILTERING

The low input voltage noise of the LMP2021/LMP2022, and no 1/f noise make these suitable for many applications with noise sensitive designs. Simple filtering can be done on the LMP2021/LMP2022 to remove high frequency noise. *Figure 3* shows a simple circuit that achieves this.

In *Figure 3* C_F and the corner frequency of the filter resulting from C_F and R_F will reduce the total noise.

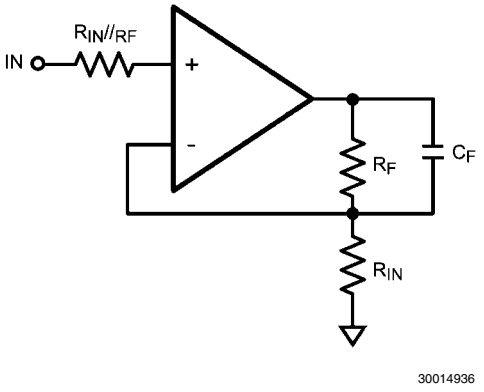

FIGURE 3. Noise Reducing Filter for Lower Gains

In order to achieve lower noise floors for even more noise stringent applications, a simple filter can be added to the op amp's output after the amplification stage. *Figure 4* shows the schematic of a simple circuit which achieves this objective. Low noise amplifiers such as the LMV771 can be used to create a single pole low pass filter on the output of the LMP2021/LMP2022. The noise performance of the filtering amplifier, LMV771 in this circuit, will not be dominant as the input signal on LMP2021/LMP2022 has already been significantly gained up and as a result the effect of the input voltage noise of the LMV771 is effectively not noticeable.

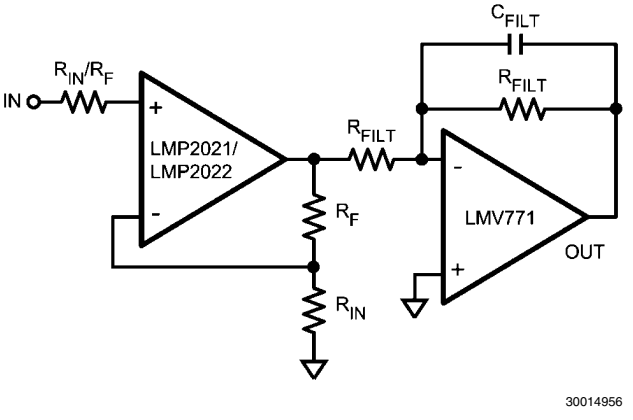

FIGURE 4. Enhanced Filter to Further Reduce Noise at Higher Gains

Using the circuit in *Figure 4* has the advantage of removing the non-linear filter bandwidth dependency which is seen when the circuit in *Figure 3* is used. The difference in noise performance of the circuits in *Figures 3*, *4* becomes apparent only at higher gains. At voltage gains of 10 V/V or less, there is no difference between the noise performance of the two circuits.

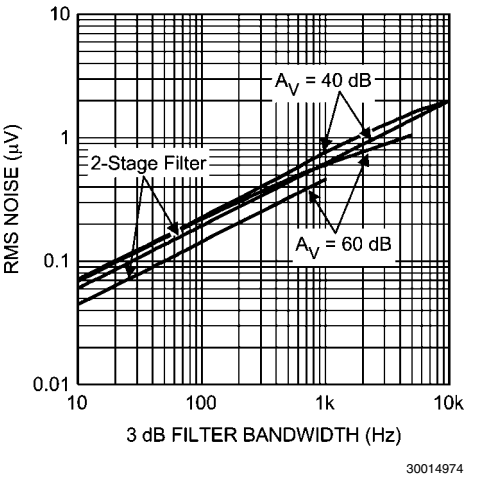

FIGURE 5. RMS Input Referred Noise vs. Frequency

Figure 5 shows the total input referred noise vs. 3 dB corner of both filters of *Figure 3* and *Figure 4* at gains of 100V/V and 1000V/V. For these measurements and using *Figure 3*'s circuit, R_F = 49.7 kΩ and R_{IN} = 497Ω. Value of C_F has been changed to achieve the desired 3 dB filter corner frequency. In the case of *Figure 4*'s circuit, R_F = 49.7 kΩ and R_{IN} = 497Ω, R_{FILT} = 49.7 kΩ, and C_{FILT} has been changed to achieve the desired 3 dB filter corner frequency. *Figure 5* compares the RMS noise of these two circuits. As *Figure 5* shows, the RMS noise measured the circuit in *Figure 4* has lower values and also depicts a more linear shape.

DIGITAL ACQUISITION SYSTEMS

High resolution ADC's with 16-bits to 24-bits of resolution can be limited by the noise of the amplifier driving them. The circuit configuration, the value of the resistors used and the source impedance seen by the amplifier can affect the noise of the amplifier. The total noise at the output of the amplifier can be dominated by one of several sources of noises such as: white noise or broad band noise, 1/f noise, thermal noise, and current noise. In low frequency applications such as medical instrumentation, the source impedance is generally low enough that the current noise coupled into it does not impact the total noise significantly. However, as the 1/f or flicker noise is paramount to many application, the use of an auto correcting stabilized amplifier like the LMP2021/LMP2022 reduces the total noise.

Table 1: RMS Input Noise Performance summarizes the input and output referred RMS noise values for the LMP2021/LMP2022 compared to that of Competitor A. As described in previous sections, the outstanding noise performance of the LMP2021/LMP2022 can be even further improved by adding a simple low pass filter following the amplification stage.

The use of an additional filter, as shown in *Figure 4* benefits applications with higher gain. For this reason, at a gain of 10, only the results of circuit in *Figure 3* are shown. The RMS input noise of the LMP2021/LMP2022 are compared with Competitor A's input noise performance. Competitor A's RMS input noise behaves the same with or without an additional filter.

Table 1: RMS Input Noise Performance

Amplifier Gain (V/V)	System Bandwidth Requirement (Hz)	RMS Input Noise (nV)		
		LMP2021/LMP2022		Competitor A
		Figure 3 Circuit	*Figure 4* Circuit	*Figures 4, 3* Circuit
10	100	229	*	300
	1000	763	*	1030
100	100	229	196	300
	1000	763	621	1030
1000	10	71	46	95
	100	158	146	300
	1000	608	462	1030

* No significant difference in Noise measurements at A_V = 10V/V

INPUT BIAS CURRENT

The bias current of the LMP2021/LMP2022 behaves differently than a conventional amplifier due to the dynamic transient currents created on the input of an auto-zero circuit. The input bias current is affected by the charge and discharge current of the input auto-zero circuit. The amount of current sunk or sourced from that stage is dependent on the combination of input impedance (resistance and capacitance), as well as the balance and matching of these impedances across the two inputs. This current, integrated in the auto-zero circuit, causes a shift in the apparent "bias current". Because of this, there is an apparent "bias current vs. input impedance" interaction. In the LMP2021/LMP2022 for an input resistive impedance of 1 GΩ, the shift in input bias current can be up to 40 pA. This input bias shift is caused by varying the input's capacitive impedance. Since the input bias current is dependent on the input impedance, it is difficult to estimate what the actual bias current is without knowing the end circuit and associated capacitive strays.

Figure 6 shows the input bias current of the LMP2021/LMP2022 and that of another commercially available amplifier from a competitor. As it can be seen, the shift in LMP2021/LMP2022 bias current is much lower than that of other chopper style or auto zero amplifiers available from other vendors.

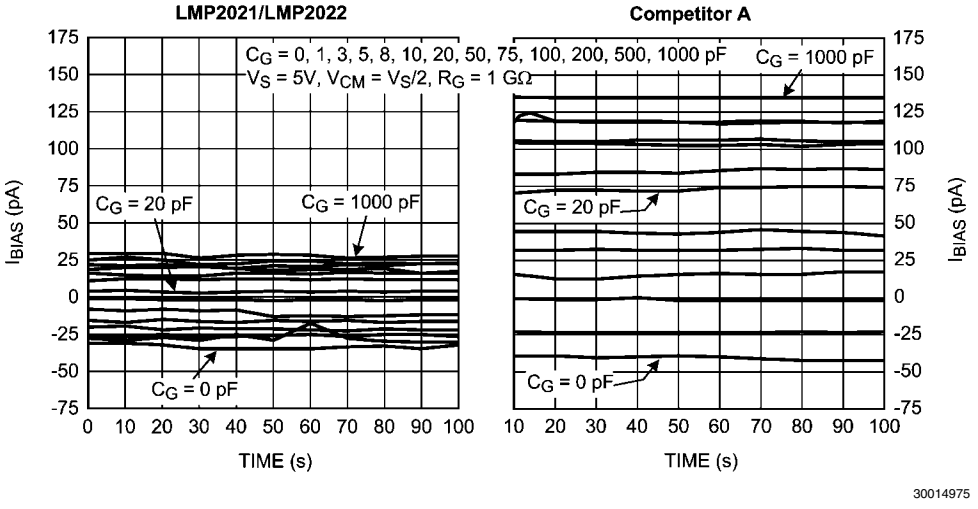

FIGURE 6. Input Bias Current of LMP2021/LMP2022 is lower than Competitor A

LOWERING THE INPUT BIAS CURRENT

As mentioned in the *INPUT BIAS CURRENT* section, the input bias current of an auto zero amplifier such as the LMP2021/LMP2022 varies with input impedance and feedback impedance. Once the value of a certain input resistance, i.e. sensor resistance, is known, it is possible to optimize the input bias current for this fixed input resistance by choosing the capacitance value that minimizes that current. *Figure 7* shows the input bias current vs. input impedance of the LMP2021/LMP2022. The value of R_G or input resistance in this test is 1 GΩ. When this value of input resistance is used, and when a parallel capacitance of 22 pF is placed on the circuit, the resulting input bias current is nearly 0 pA. *Figure 7* can be used to extrapolate capacitor values for other sensor resistances. For this purpose, the total impedance seen by the input of the LMP2021/LMP2022 needs to be calculated based on *Figure 7*. By knowing the value of R_G, one can calculate the corresponding C_G which minimizes the non-inverting input bias current, positive bias current, value.

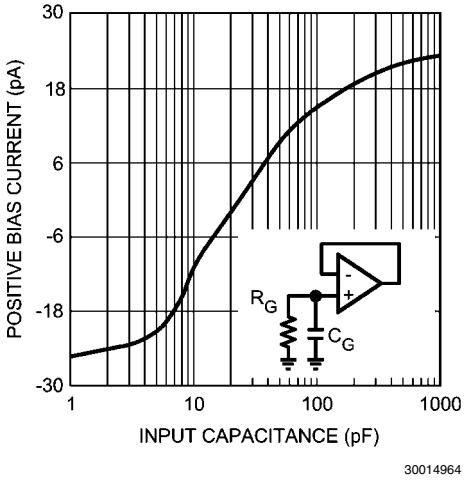

FIGURE 7. Input Bias Current vs. C_G with R_G = 1 GΩ

In a typical I-V converter, the output voltage will be the sum of DC offset plus bias current and the applied signal through the feedback resistor. In a conventional input stage, the inverting input's capacitance has very little effect on the circuit. This effect is generally on settling time and the dielectric soakage time and can be ignored. In auto zero amplifiers, the input capacitance effect will add another term to the output. This additional term means that the baseline reading on the output will be dependent on the input capacitance. The term input capacitance for this purpose includes circuit strays and any input cable capacitances. There is a slight variation in the capacitive offset as the duty cycle and amplitude of the pulses vary from part to part, depending on the correction at the time. The lowest input current will be obtained when the impedances, both resistive and capacitive, are matched between the inputs. By balancing the input capacitances, the effect can be minimized. A simple way to balance the input impedance is adding a capacitance in parallel to the feedback resistance. The addition of this feedback capacitance reduces the bias current and increases the stability of the operational amplifier. *Figure 8* shows the input bias current of the LMP2021/LMP2022 when R_F is set to 1 GΩ. As it can be seen from *Figure 8*, choosing the optimum value of C_F will help reducing the input bias current.

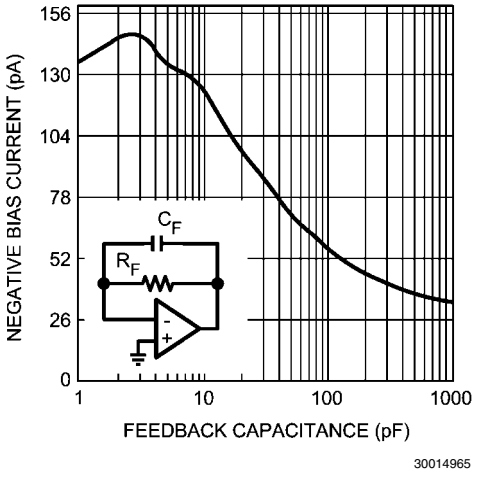

FIGURE 8. Input Bias Current vs. C_F with R_F = 1 GΩ

The effect of bias current on a circuit can be estimated with the following:

$$A_V * I_{BIAS+} * Z_S - I_{BIAS-} * Z_F$$

Where A_V is the closed loop gain of the system and I_{BIAS+} and I_{BIAS-} denote the positive and negative bias current, respectively. It is common to show the average of these bias currents in product datasheets. If I_{BIAS+} and I_{BIAS-} are not individually specified, use the I_{BIAS} value provided in datasheet graphs or tables for this calculation.

For the application circuit shown in *Figure 12*, the LMP2022 amplifiers each have a gain of 18. With a sensor impedance of 500Ω for the bridge, and using the above equation, the total error due to the bias current on the outputs of the LMP2022 amplifier will be less than 200 nV.

SENSOR IMPEDANCE

The sensor resistance, or the resistance connected to the inputs of the LMP2021/LMP2022, contributes to the total impedance seen by the auto correcting input stage.

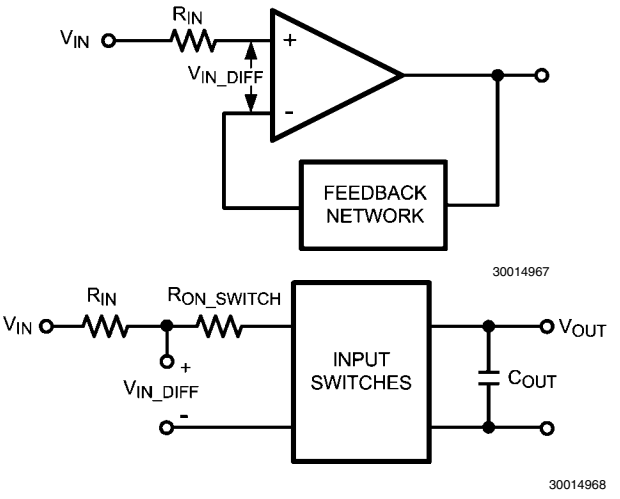

FIGURE 9. Auto Correcting Input Stage Model

As shown in *Figure 9*, the sum of R_{IN} and $R_{ON-SWITCH}$ will form a low pass filter with C_{OUT} during correction cycles. As R_{IN} increases, the time constant of this filter increases, resulting in a slower output signal which could have the effect of reducing the open loop gain, A_{VOL}, of the LMP2021/LMP2022. In order to prevent this reduction in A_{VOL} in presence of high impedance sensors or other high resistances connected to the input of the LMP2021/LMP2022, a capacitor can be placed in parallel to this input resistance. This is shown in *Figure 10*

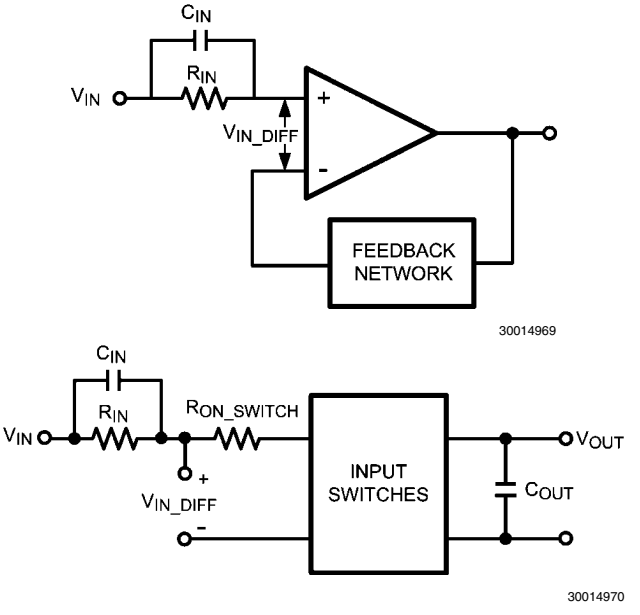

FIGURE 10. Sensor Impedance with Parallel Capacitance

C_{IN} in *Figure 10* adds a zero to the low pass filter and hence eliminating the reduction in A_{VOL} of the LMP2021/LMP2022. An alternative circuit to achieve this is shown in *Figure 11*.

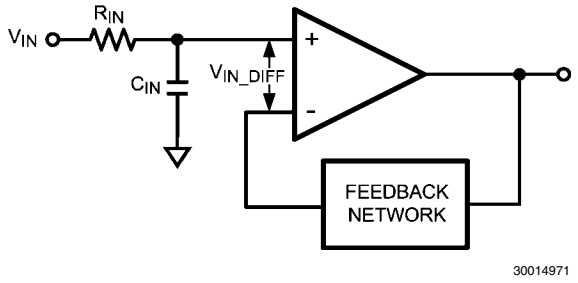

FIGURE 11. Alternative Sensor Impedance Circuit

TRANSIENT RESPONSE TO FAST INPUTS

On chip continuous auto zero correction circuitry eliminates the 1/f noise and significantly reduces the offset voltage and offset voltage drift; all of which are very low frequency events. For slow changing sensor signals this correction is transparent. For excitations which may otherwise cause the output to swing faster than 40 mV/µs, there are additional considerations which can be viewed two perspectives: for sine waves and for steps.

For sinusoidal inputs, when the output is swinging rail-to-rail on ±2.5V supplies, the auto zero circuitry will introduce distortions above 2.55 kHz. For smaller output swings, higher frequencies can be amplified without the auto zero slew limitation as shown in table below. Signals above 20 kHz, are not affected, though normally, closed loop bandwidth should be kept below 20 kHz so as to avoid aliasing from the auto zero circuit.

$V_{OUT-PEAK}$ (V)	$f_{MAX-SINE\ WAVE}$ (kHz)
0.32	20
1	6.3
2.5	2.5

For step-like inputs, such as those arising from disturbances to a sensing system, the auto zero slew rate limitation manifests itself as an extended ramping and settling time, lasting ~100 µs.

DIFFERENTIAL BRIDGE SENSOR

Bridge sensors are used in a variety of applications such as pressure sensors and weigh scales. Bridge sensors typically have a very small differential output signal. This very small signal needs to be accurately amplified before it can be fed into an ADC. As discussed in the previous sections, the accuracy of the op amp used as the ADC driver is essential to maintaining total system accuracy.

The high DC performance of the LMP2021/LMP2022 make these amplifiers ideal choices for use with a bridge sensor. The LMP2021/LMP2022 have very low input offset voltage and very low input offset voltage drift. The open loop gain of the LMP2021/LMP2022 is 160 dB.

The on chip EMI rejection filters available on the LMP2021/LMP2022 help remove the EMI interference introduced to the signal and hence improve the overall system performance.

The circuit in *Figure 12* shows a signal path solution for a typical bridge sensor using the LMP2021/LMP2022. Bridge sensors are created by replacing at least one, and up to all four, of the resistors in a typical bridge with a sensor whose resistance varies in response to an external stimulus. Using four sensors has the advantage of increasing output dynamic range. Typical output voltage of one resistive pressure sensor is 2 mV per 1V of bridge excitation voltage. Using four sensors, the output of the bridge is 8 mV per 1V. The bridge voltage is this system is chosen to be 1/2 of the analog supply voltage and equal to the reference voltage of the ADC161S626, 2.5V. This excitation voltage results in 2.5V * 8 mV = 20 mV of differential output signal on the bridge. This 20 mV signal must be accurately amplified by the amplifier to best match the dynamic input range of the ADC. This is done by using one LMP2022 and one LMP2021 in front of the ADC161S626. The gaining of this 20 mV signal is achieved in 2 stages and through an instrumentation amplifier. The LMP2022 in *Figure 12* amplifies each side of the differential output of the bridge sensor by a gain 18. Bridge sensor measurements are usually done up to 10s of Hz. Placing a 300 Hz filter on the LMP2022 helps removing the higher frequency noise from this circuit. This filter is created by placing two capacitors in the feedback path of the LMP2022 amplifiers. Using the LMP2022 with a gain of 18 reduces the input referred voltage noise of the op amps and the system as a result. Also, this gain allows direct filtering of the signal on the LMP2022 without compromising noise performance. The differential output of the two amplifiers in the LMP2022 are then fed into a LMP2021 configured as a difference amplifier. This stage has a gain of 5, with a total system having a gain of (18*2+1)*5 = 185. The LMP2021 has an outstanding CMRR value of 139. This impressive CMRR improves system performance by removing the common mode signal introduced by the bridge. With an overall gain of 185, the 20 mV differential input signal is gained up to 3.7V. This utilizes the amplifiers output swing as well as the ADC's input dynamic range.

This amplified signal is then fed into the ADC161S626. The ADC161S626 is a 16-bit, 50 kSPS to 250 kSPS 5V ADC. In order to utilize the maximum number of bits of the ADC161S626 in this configuration, a 2.5V reference voltage is used. This 2.5V reference is also used to power the bridge sensor and the inverting input of the ADC. Using the same voltage source for these three points helps reducing the total system error by eliminating error due to source variations.

With this system, the output signal of the bridge sensor which can be up to 20 mV is accurately gained to the full scale of the ADC and then digitized for further processing. The LMP2021/LMP2022 introduced minimal error to the system and improved the signal quality by removing common model signals and high frequency noise.

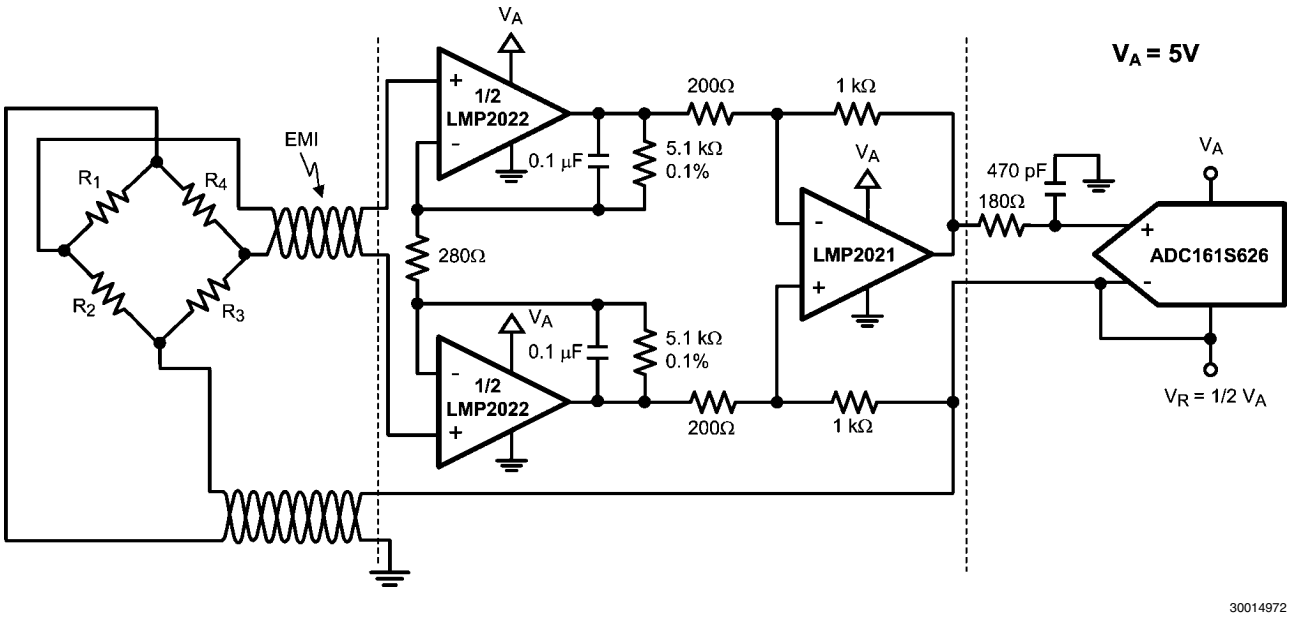

FIGURE 12. LMP2021/LMP2022 used with ADC161S626

Physical Dimensions inches (millimeters) unless otherwise noted

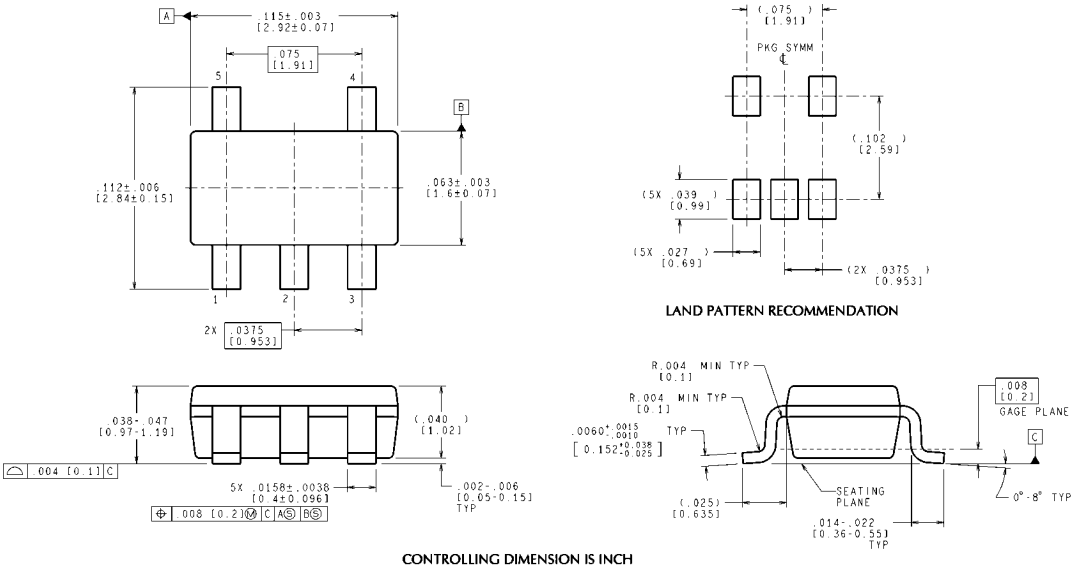

CONTROLLING DIMENSION IS INCH
VALUES IN [ ] ARE MILLIMETERS
DIMENSIONS IN ( ) FOR REFERENCE ONLY

MF05A (Rev D)

5-Pin SOT-23
NS Package Number MF05A

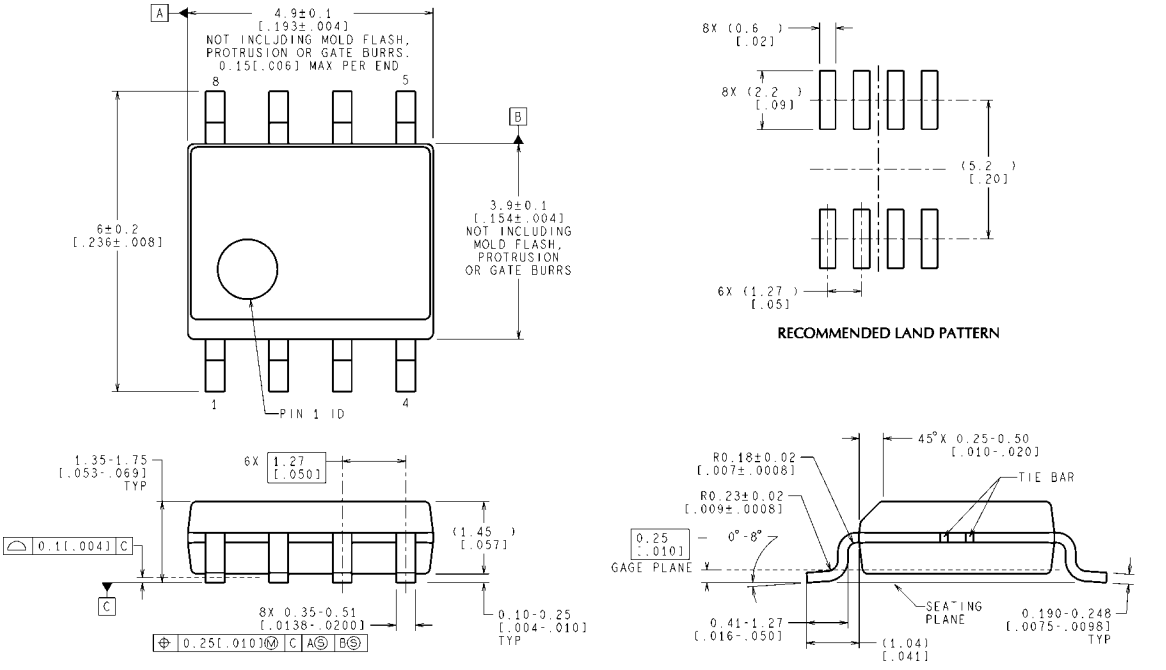

CONTROLLING DIMENSION IS MILLIMETER
VALUES IN [ ] ARE INCHES
DIMENSIONS IN ( ) FOR REFERENCE ONLY

M08A (Rev M)

8-Pin SOIC
NS Package Number M08A

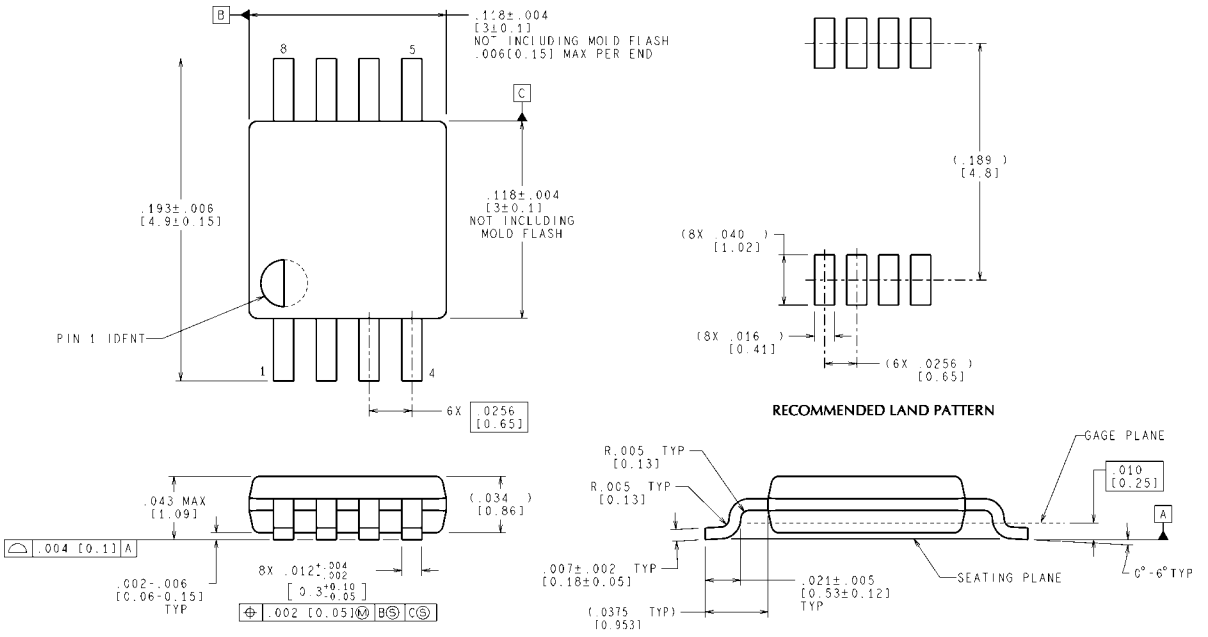

CONTROLLING DIMENSION IS INCH
VALUES IN [ ] ARE MILLIMETERS

MUA08A (Rev F)

8-Pin MSOP
NS Package Number MUA08A

Notes

For more National Semiconductor product information and proven design tools, visit the following Web sites at:

Products		Design Support	
Amplifiers	www.national.com/amplifiers	WEBENCH® Tools	www.national.com/webench
Audio	www.national.com/audio	App Notes	www.national.com/appnotes
Clock and Timing	www.national.com/timing	Reference Designs	www.national.com/refdesigns
Data Converters	www.national.com/adc	Samples	www.national.com/samples
Interface	www.national.com/interface	Eval Boards	www.national.com/evalboards
LVDS	www.national.com/lvds	Packaging	www.national.com/packaging
Power Management	www.national.com/power	Green Compliance	www.national.com/quality/green
Switching Regulators	www.national.com/switchers	Distributors	www.national.com/contacts
LDOs	www.national.com/ldo	Quality and Reliability	www.national.com/quality
LED Lighting	www.national.com/led	Feedback/Support	www.national.com/feedback
Voltage Reference	www.national.com/vref	Design Made Easy	www.national.com/easy
PowerWise® Solutions	www.national.com/powerwise	Solutions	www.national.com/solutions
Serial Digital Interface (SDI)	www.national.com/sdi	Mil/Aero	www.national.com/milaero
Temperature Sensors	www.national.com/tempsensors	SolarMagic™	www.national.com/solarmagic
Wireless (PLL/VCO)	www.national.com/wireless	PowerWise® Design University	www.national.com/training

National Semiconductor Americas Technical Support Center
Email: support@nsc.com
Tel: 1-800-272-9959

National Semiconductor Europe Technical Support Center
Email: europe.support@nsc.com

National Semiconductor Asia Pacific Technical Support Center
Email: ap.support@nsc.com

National Semiconductor Japan Technical Support Center
Email: jpn.feedback@nsc.com